Simulation Models for Intraparticle Deactivation: Scope and Reliability

D. M. DOWNING
J. W. LEE
and
J. B. BUTT

Department of Chemical Engineering
and
Ipatieff Catalytic Laboratory
Northwestern University
Evanston, Illinois 60201

An experimental and modeling study of the dynamic behavior of an individual catalyst pellet as influenced by deactivation and dilution has been made. The reaction system employed was benzene hydrogenation over nickel/kieselguhr catalyst pellets diluted with 10% graphite, 10% silica, or undiluted; thiophene was employed as the catalyst poison.

A one-dimensional effective transport model was developed, and the parameters for this model were determined principally from separate off line experiments or steady state experimental information. The adequacy of the model was determined from a direct comparison of the experimental and computed time-temperature profiles.

SCOPE

The application of simulation models to the transient response of fresh and deactivated catalyst particles, differing in physical properties, is treated. Benzene hydrogenation over a nickel/kieselgehr catalyst, poisoned by thiophene is used as an experimental example of the class of exothermic catalytic reactions subject to irreversible poisoning. The catalysts investigated included formulations diluted with silica or graphite as well as the original material and exhibited a range of physical properties.

Major objectives of the study are investigations of the feasibility of completely a priori simulations (all parameters determined independently) to the extreme case of transient response represented by start-up of the fresh and deactivated catalyst, the effort required to obtain a given level of detail in simulation, and the parametric sensitivity of such catalyst reaction-poison systems.

CONCLUSIONS AND SIGNIFICANCE

Steady state and transient response behavior are strongly influenced by catalyst deactivation. A full distributed parameter model, described previously, was used to simulate the transient response of fresh and deactivated catalyst pellets possessing differing intraparticle transport properties. Attempts at full a priori simulation at the highest level of detail (spatial and temporal variation of intraparticle temperature profiles) were not successful. Investigation of the parametric response of the model revealed extreme sensitivity to the pellet intraparticle diffusivity and external heat transfer coefficient. Both the full model and simplified versions employing an active shell (undeactivated pellet) or a dead zone (deactivated pellet) at the surface could be used for successful simulation of the experimentally observed behavior, but only in the sense of parameter fit models.

It would appear that global, averaged quantities such as steady state activity and overall rates of deactivation can be simulated using a priori parameter sets; however, detailed simulations apparently require parameters to be known to an accuracy beyond current capabilities in estimation or measurement.

In a recent paper (Lee et al., 1978), we reported on the computer simulation of a series of experiments dealing with the steady state and transient behavior of partially deactivated catalyst particles for the hydrogenation of benzene. The simulation was attempted on an a priori basis in that all model parameters such as kinetic coefficients and transport properties were determined either in separate, off line experiments or from steady state measurements on the catalyst particle itself. In general the results of these confrontations of simulation (essentially the calculation of intraparticle and interphase temperature profiles) with experiment have been satisfactory for the steady state and transients in unactivated catalysts, somewhat less satisfactory for deactivated particles. Nagging doubts persist even for our most successful simulations, however, since it was always necessary to make adjustments to the value of intraparticle transport parameters to obtain the best fit.

This experience has led us to pose some questions about the simulations themselves, since it is not clear what effort is required to attain a simulation model that is satisfactory to a specified degree. In particular, we ask what is the permitted accumulation of experimental uncertainty in parametric values and how do uncertainties in different parameters interact with each other. Further, what econ-

Correspondence concerning this paper should be addressed to J. B. Butt. D. M. Downing is with Exxon Research and Engineering Laboratories, Baton Rouge, Louisiana 70821. J. W. Lee is with Mobil Research and Development Corp., Paulsboro, New Jersey 08065.

0001-1541-79-2497-0461-$01.05.

Table 1. Catalyst Pellet Parameters

Property	Undiluted (NK)	Diluted (NKS)	Diluted (NKG)
Density, g/cm³	1.693	1.478	1.589
Length, cm	5.95	6.40	6.88
Diameter, cm	1.28	1.29	1.28
Weight, g	12.93	12.40	14.04
Heat capacity, J/g-°C[a]	0.619	0.636	0.603
Microporosity[b]	0.197	0.048	0.061
Micropore radius, nm	6.3	8.5	7.1
Macroporosity	0.286	0.549	0.395
Macropore radius, nm	60.0	117.0	50.4
Effective diffusivity,	1.7[c]	—	—
$cm^2/s \times 10^2$	3.2[d]	4.7	2.8
	3.5[e]	5.6	1.5
Thermal conductivity,	18.0[f]		
$J/cm\text{-}s\text{-}°C \times 10^4$	33.3[g]	18.0	70.3[g]

[a] Computed from tabulated values for individual components as given in the International Critical Tables.
[b] Pore size distribution determined by mercury porosimetry courtesy of Dr. F. G. Dwyer, Mobil Research and Development Corporation.
[c] Computed from experimental temperature profile data using the equation of Prater (1958) and a thermal conductivity of 17.6×10^{-4} J/cm-s-°C.
[d] Measured via He-N_2 counterdiffusion at 25°C and 1 atm courtesy of Dr. K. K. Robinson, Amoco Oil Company. Corrected for reaction conditions.
[e] Computed from the random pore model (Wakao and Smith, 1962).
[f] Measured by thermal comparator method (Lee, 1976).
[g] Computed from experimental temperature profile data using the equation of Prater (1958) and the effective diffusivities determined by counterdiffusion, corrected for reaction conditions.

omies in simulation are permitted if, for example, one is interested in determining only global activity rather than detailed shapes of temperature profiles? In what follows we shall be concerned with modeling the intraparticle deactivation problem in particular; however, the information presented should be of more general application to any reaction engineering problem involving steep gradients which change in spatial position with time.

EXPERIMENTAL

The basic experimental information obtained is intraparticle and interphase temperature gradients in a single pellet reactor; hydrogenation of benzene on nickel/kieselguhr is the test reaction employed, and thiophene is used as a catalyst poison. Most measurements were obtained in a start-up experiment, described in detail previously (Lee et al., 1978) in which a fresh or partially deactivated catalyst pellet initially in flowing hydrogen is subjected to a step input in benzene concentration to the reactor. Catalysts were deactivated either by introduction of thiophene with the benzene feed under steady state conditions or by introduction with the feed in a start-up experiment.

Since this work had as a major concern the influence of parametric values on system response and simulation two pellets, composed of 90% nickel/kieselguhr and 10% of either graphite or silica, were investigated in addition to the undiluted material studied by Lee (1976). The addition of diluent affects the catalyst pellet by changing the rate of reaction per unit volume of material and varying the thermal conductivity and heat capacity. In the present case, addition of silica has only a small effect on thermal conductivity, since that material is similar to kieselguhr while the graphite increases conductivity markedly (Kehoe and Butt, 1972*b*). The motivation for the modification of thermal conductivity lies in part on computational work reporting the significant effect of variations in the Lewis number $\lambda_e/(\rho C_p)_{cat}/D_e$ on the transient behavior of the nonisothermal catalyst pellet (Lee and Luss, 1969, 1970). Of course, addition of diluent also changes the internal pore structure of the pellets which may influence the diffusion coefficient, so in effect it is the ratio (λ_e/D_e) which is involved in changes in the Lewis number.

Properties of the catalyst pellets are given in Table 1. The transport properties have been evaluated by a number of methods, as indicated; while different methods yield the same order of magnitude values, there remains considerable discrepancy if one is concerned about absolute magnitude. This will be seen to have important consequences in simulation.

MODEL AND PARAMETERS

The single-pellet reactor has been described previously (Lee et al., 1978; Kehoe and Butt, 1972*b*); the essential feature of the design is conformity to the model of an infinitely long, radially symmetric, catalyst particle bathed in a reaction mixture of uniform composition. The catalyst pellet properties are taken to be isotropic, interphase gradients are modeled using film theory approximations, and all properties other than catalyst activity are considered independent of the extent of deactivation. The deactivation kinetics are modeled by a separable rate form, and there is a linear relationship between the fraction of sites available for hydrogenation and the amount of thiophene adsorbed on the catalyst. Hydrogen is present in large excess in the experiments, so a mass conservation relation for it is not included in the model.

The benzene hydrogenation reaction is known to be reversible at higher temperatures, the reverse reaction becoming significant at temperatures greater than about 220°C. The irreversible kinetic model employed here is adequate so long as experimental comparisons are restricted to temperatures below about 190°C, which has been done.

The full model is then assembled from the following components. Rate of benzene hydrogenation (Kehoe and Butt, 1972*a*):

$$-r_B = \frac{a \exp(-F/RT) C_B}{1 + b \exp(H/RT)\, C_B} \tag{1}$$

Rate of change of active sites:

$$-r_D = k_d{}^0 \exp(-E_D/RT) s = ds/dt \tag{2}$$

Rate of thiophene adsorption:

$$r_T = M_T r_D \tag{3}$$

Mass conservation, benzene, cyclohexane, thiophene:

$$\frac{\partial C_B}{\partial t} = D_e \nabla^2 C_B - s r_B \tag{4}$$

$$\frac{\partial C_C}{\partial t} = D_e \nabla^2 C_C + s r_B \tag{5}$$

$$\frac{\partial C_T}{\partial t} = D_e \nabla^2 C_T + \rho r_T \tag{6}$$

Energy conservation:

$$\frac{\partial T}{\partial t} = \lambda_e \nabla^2 T + (-\Delta H)\, s r_B \tag{7}$$

Initial conditions:

$$T = T_i(r) \tag{8}$$

$$s = 1 \text{ (fresh) or } s(r) \text{ (deactivated)} \tag{9}$$

$$C_i = C_{i0}(r) \quad i = B, C, T \tag{10}$$

Boundary conditions:

TABLE 2. KINETIC PARAMETERS

1. Benzene hydrogenation

$a = 1.02 \times 10^4\ s^{-1}$
$b = 1.70 \times 10^{-4}\ m^3/mole$
$F = 1.20 \times 10^4\ J/mole$
$H = 3.68 \times 10^4\ J/mole$

2. Thiophene poisoning

$k_d^o = 4.09 \times 10^{-1}\ m^3/mole\text{-}s$
$E_D = 4.52 \times 10^3\ J/mole$
$M_T = 5.0 \times 10^{-4}\ mole/g$

TABLE 3. HEAT TRANSFER COEFFICIENTS

Run*	$h_T \times 10^4$, J/cm²-s-°C
NKG F65	47.2
NKG F110	65.6
NKG D65	37.7
NKG D110	43.8
NKS F65	38.5
NKS F110	51.0
NKS D65	38.9
NKS D110	39.6
6U1	28.3

* Run notation: NKG–Harshaw Ni–0104 P + 10% Superior Graphite, #2134; NKS–Harshaw Ni–0104 P + 10% Fisher C211 Silica. F = fresh catalyst; D–deactivated catalyst; 65,110–feed temperature, °C.

TABLE 4. EXPERIMENTAL RUNS*

Run ID†	T_F °C	% diluent**	S††	Source
NKG-F65	65	10%-Gr	1.0	Downing (1977)
NKG-F110	110	10%-Gr	1.0	Downing (1977)
NKG-P65	65	10%-Gr	SP	Downing (1977)
NKG-D65	65	10%-Gr	0.22	Downing (1977)
NKG-D110	110	10%-Gr	0.35	Downing (1977)
NKS-F65	65	10%-Si	1.0	Downing (1977)
NKS-F110	110	10%-Si	1.0	Downing (1977)
NKS-P65	65	10%-Si	SP	Downing (1977)
NKS-D65	65	10%-Si	0.36	Downing (1977)
NKS-D110	110	10%-Si	0.52	Downing (1977)
6U1	65	0%	1.0	Lee (1976)
6U2	65	0%	0.40	Lee (1976)
6PP8-1	65	0%	0.16	Lee (1976)
1SJ	110	0%	1.0	Lee (1976)

* For all experimental runs, total flow rate is 31/min (S.C.), mole fraction of benzene is 0.16, and mole fraction of thiophene for poisoning runs is 0.0018.
† Run notation: NKS–silica diluted; NKG–graphite diluted, 6U, 6PP–undiluted. 65 or 110–feed temperatures, °C.
** Gr = graphite, Si = silica.
†† SP = start-up poisoning run.

$$\nabla C_i = \nabla T = 0, \quad r = 0 \tag{11}$$

$$D_e\left(\frac{\partial C_i}{\partial r}\right)_{R_p} = k_g\,[C_{i0}(t) - C_i] \tag{12}$$

$$\lambda_e\left(\frac{\partial T}{\partial r}\right)_{R_p} = h_T\,[T_B(t) - T] \tag{13}$$

A dimensionless form of this set of coupled nonlinear parabolic equations was solved numerically using the Crank-Nicolson finite-difference method and the Thomas algorithm to invert the resulting tridiagonal matrices (Downing, 1977).

Aside from the pellet parameters given in Table 1, the model above contains those parameters associated with the kinetic correlations for the main and poisoning reactions, the poison capacity parameter M_T, and the mass and heat transfer coefficients. The means for securing kinetic parameters has been detailed previously (Kehoe and Butt, 1972*a*), and no further discussion is given here; pertinent values are given in Table 2.

The film heat transfer coefficients in this work were determined directly from experimental steady state data using the steady state energy balance over the pellet:

$$h_T = \frac{(-\Delta H)\Omega}{a'\Delta T_x} \tag{14}$$

In Table 3 are given the values of heat transfer coefficients so determined for the experimental runs. These values are dependent upon an accurate measurement of the interphase temperature difference ΔT_x. The results from a steady state analysis of the experimental runs of Lee (1976) by Butt et al. (1977) would support the use of steady state balances on the pellet for this purpose and suggest that the experimentally measured temperature differences are accurately determined.

The corresponding mass transfer coefficients were determined from correlations for the ratio of mass and heat Biot numbers utilizing standard j factor correlations for heat and mass transfer. Carberry (1966) has suggested that a good approximation for most systems is realized by $j_D = j_H$ and $N_{Sc} = N_{Pr}$. In this case, the ratio of Biot numbers is given by

$$r = \frac{N_{BiM}}{N_{Bih}} = \frac{\lambda_e}{D_e} \cdot \frac{1}{(\rho C_p)_g} \tag{15}$$

This form of correlation has evolved from forms developed for fixed beds but has been employed successfully in several single-pellet flow configurations (Benham and Denny, 1972; Koh and Hughes, 1974; Carberry, 1975).

EXPERIMENTAL RESULTS AND DISCUSSION

The effects of deactivation are investigated here using an experimental procedure in which the behavior of the fresh catalyst pellet is first characterized, after which the pellet is partially deactivated and the experiments repeated. Comparisons can be drawn here between the fresh and deactivated pellets as well as the diluted and undiluted cases. The results so compared are the observed global rate of reaction at steady state, the shape and magnitude of the intraparticle temperature profile, and the magnitude of the time required for the system to attain steady state in start-up. A selection of experimental conditions representative of the overall investigation of Downing (1977) is used for purposes of illustration here and is given in Table 4. In addition, undiluted pellet data reported by Lee (1976) are included for comparison of the effects of changes in the physical properties of the pellets. The global activity parameter S listed in Table 4 is the ratio of the overall rate of reaction for the deactivated pellet to that for the fresh pellet.

Undeactivated Pellets, Low Temperature (65°C)

The start-up behavior of both graphite and silica diluted pellets was similar, as shown in Figure 1, although with about a 25% difference in time required to attain steady state. A slightly higher final temperature was attained by the NKG pellet, with a correspondingly higher final rate of reaction, 3.8 $\times 10^{-6}$ gmole/g-s (NKG) vs. 3.4 $\times 10^{-6}$ gmole/g-s (NKS). Note that there is indication of a small intraparticle temperature gradient for the NKS pellet, absent in the NKG pellet. This can be attributed to the difference in thermal conductivity between the two. There is an experimental problem in identifying the exact time at which the pellet reaches a thermal steady state owing to the discrete time measurement of the

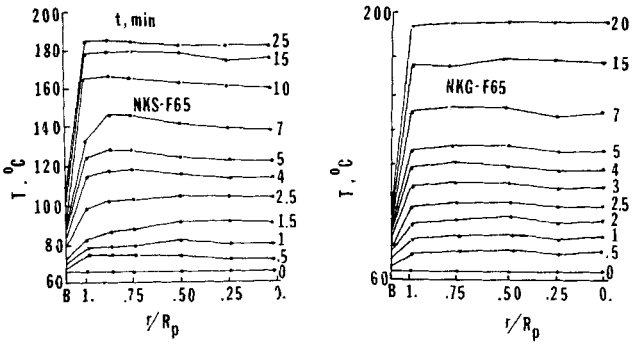

Fig. 1. Start-up behavior of silica and graphite diluted pellets at low temperature.

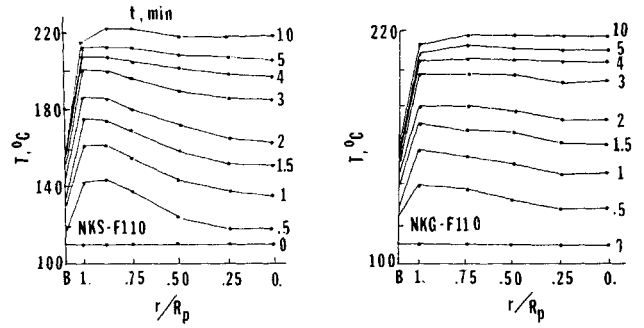

Fig. 3. Start-up behavior of silica and graphite diluted pellets at high temperature.

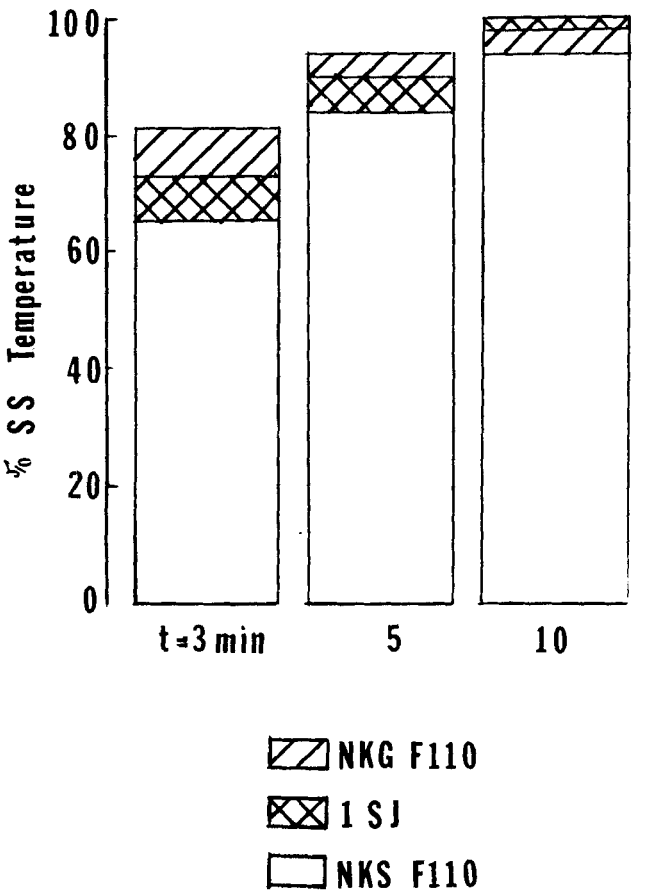

Fig. 4. Temperature approach to steady state, high temperature runs for all catalysts.

temperature. To circumvent this, we have plotted the ratio of the difference between the temperature at time t and the initial temperature to the difference between final steady state temperature and initial temperature as a function of time. The

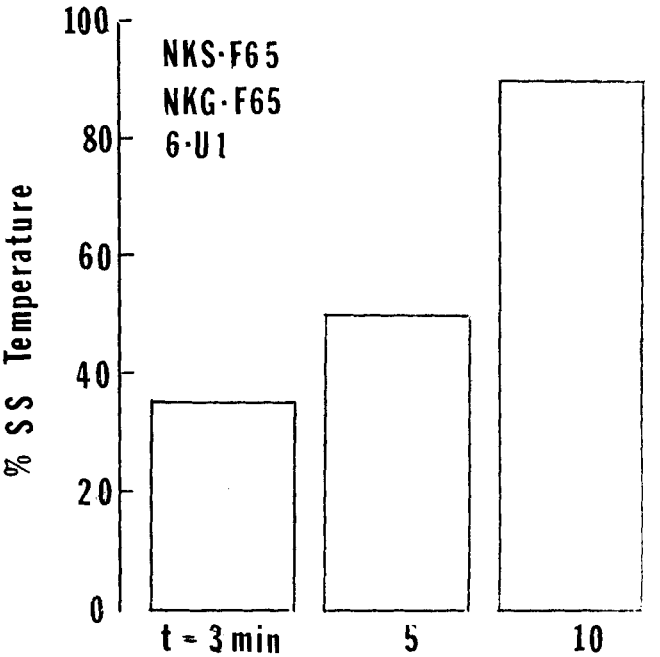

Fig. 2. Temperature approach to steady state, low temperature runs for all catalysts.

temperature at the dimensionless radial position 0.5 is used for this purpose; other positions were investigated and found to give similar results. Such a plot is given in Figure 2 for the low temperature runs; differences between NKG and NKS were less than 1%, so the single bar graph represents the behavior of both systems (indeed, the behavior of the undiluted pellet 6U1 is also represented by this graph). It is seen that the system is over 50% of the way to steady state within the first 25% of the time scale of the response.

Undeactivated Pellets, High Temperature

Corresponding start-up results at the higher feed temperature (110°C) are shown in Figures 3 and 4. In this case, the final steady temperatures are essentially the same for NKG, NKS, and the undiluted pellet; the final reaction rate essentially the same, 3.7×10^{-6} vs. 3.5×10^{-6} for NKG, NKS; but the time response differs among the individual pellets and is qualitatively different from the low temperature runs (Figures 2 and 4). At high temperatures all the benzene is reacted at or near the surface in an annular region, and a temperature maximum remains near the surface until the attainment of steady state. At lower temperatures the temperature maximum appears first at the surface, then moves toward the center of the pellet, and finally returns to the surface during the course of the experiment. This wandering hot spot, observed here for NKS, has been reported before (Lee et al., 1978) and is the result of differing characteristic rates of mass and heat transport within the pellet. Since the Lewis number is nearly independent of temperature, the observed differences in low and high temperature response would not be expected on the basis of this measure alone.

It is interesting to note that 10% graphite dilution in the present case does not eliminate the development of intraparticle temperature gradients (although they are considerably reduced in magnitude). Lee (1976) and Kehoe (1971) report complete isothermality for similar pellets diluted with 20 and 25% graphite, respectively.

Deactivated Pellets, Low and High Temperatures

Start-up experiments were run on partially deactivated pellets for purposes of comparison with the fresh pellet behavior. The conditions of deactivation were either at 65° or 110°C, with $x_T = 0.0018$, $x_B = 0.16$, and time of 15 min. Figures 5 and 6 present the results for both temperature levels. As expected, the deactivation modifies the global rate of reaction, the magnitude of the steady state temperature profile, and the time required to attain steady state. As shown by the global

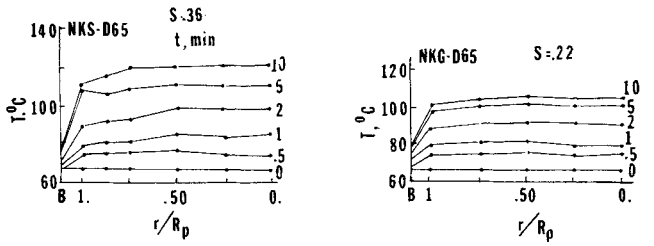

Fig. 5. Time-temperature profiles for low temperature runs with deactivated catalysts.

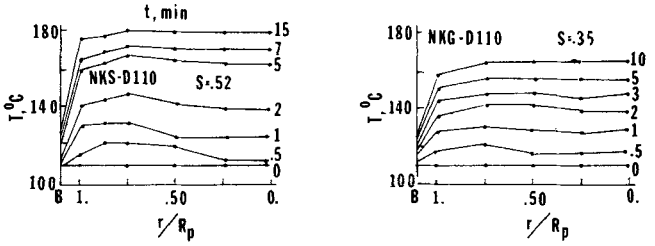

Fig. 6. Time-temperature profiles for high temperature runs with deactivated catalysts.

activity variable S, the NKG pellet is more severely affected by deactivation under these conditions, an interesting observation which would not be expected on the basis of relative porosities or effective diffusivities (Table 1). The time to reach steady state is illustrated in Figure 7. For 3 min into the experiment for NKS-D65, 67% of the overall change has taken place, compared with only 36% for NKS-F65. However, the responses of NKS-F110 and NKS-D110 were quite similar, as shown in the figure. The temperature response patterns observed for fresh and deactivated NKG were similar to those for NKS, including the differences between low and high temperature patterns.

Start-up Poisoning Experiments

Start-up types of experiments, in which the feed contained thiophene, were also used to deactivate both types of pellet. Conditions and time of deactivation were identical to the steady state prepoisoning used in the runs described above. Now in steady state poisoning it could be assumed that deactivation would be influenced by higher temperature and corresponding high rate of reaction, resulting in a shallow benzene and thiophene penetrations into the pellet. In contrast, the start-up poisoning experiment would be characterized by lower temperatures, at least initially, with consequently deeper initial penetrations of reactant and poison into the pellet. However, under identical conditions, the resulting global activity levels for the two types of experiments were very similar: 0.36 in both for NKS (65°C) and 0.22 vs. 0.26 for NKG (65°C). These results suggest that the poisoning can be described by a progressive shell model, where the reactants and poison do not penetrate far into the active pellet under any of the conditions employed here, and the poisoning and main reactions compete for the same surface sites located in the outer portion of the pellet.

Summary

In general, the diluted pellets are similar to each other in their behavior, and the general characteristics of the transients are also qualitatively similar to those reported for the undiluted pellet (Lee et al., 1978). Such similarity can be attributed to the fact that in all cases the reaction zone is confined to a relatively small volume near the external surface of the pellet, even though there is variation among the properties of the individual pellets. Consequently, it is important to establish the physical properties of this zone in comparison of those for the entire pellet. Of particular importance in the present investigation are possible localized nonuniformities in density and effective diffusivity near the surface. The variation in these properties, particularly in the region at or near the surface, may be critical in defining the overall response characteristics observed experimentally.

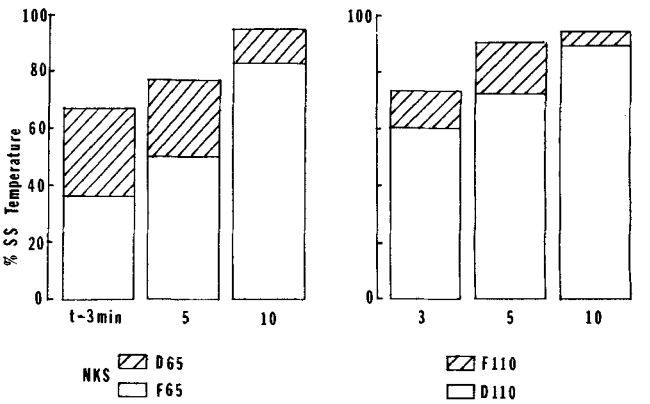

Fig. 7. Temperature approach to steady state; comparison between fresh and deactivated NKS catalysts at both low and high temperatures.

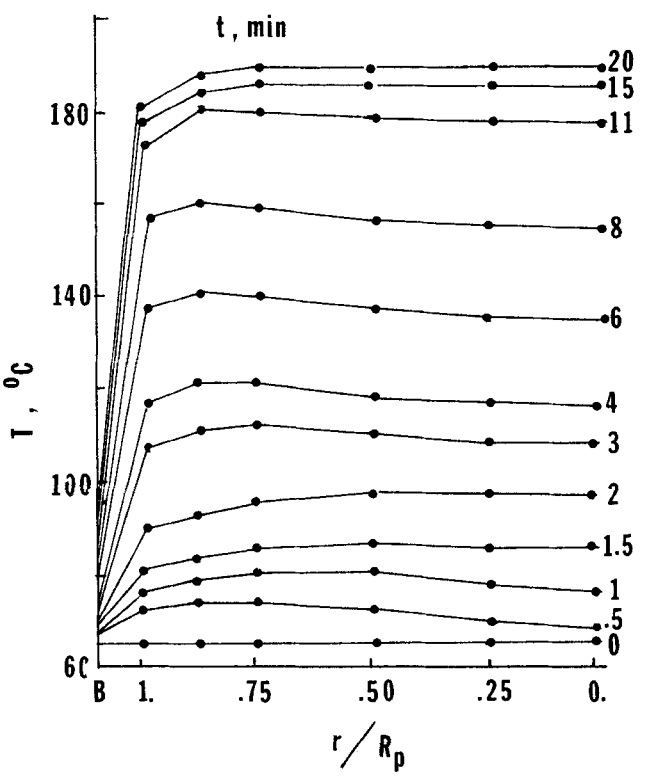

Fig. 8. Start-up response for the fresh, undiluted pellet, run 6U1.

SIMULATION RESULTS AND DISCUSSION

The objective in simulation is not only to model experimentally measured temperature profiles but also to elucidate the relationship between the computational effort and the various levels of detail possible. The experimental runs (fresh, deactivated, poisoning, nonpoisoning) are interconnected in the sense that the problems of simulation posed by each are solved in the same order as the experiments were conducted, with each solution building on information from the preceding problem. The objectives of each case are as follows:

1. Nondeactivated: to establish a feasible parameter set and level of modeling for uncontaminated feed.
2. Poisoning: to evaluate the poisoning model in terms of its ability to predict a time varying activity profile as the pellet is being poisoned by contaminated feed.
3. Deactivated: to examine the requirements needed to simulate the temperature response of the poisoned

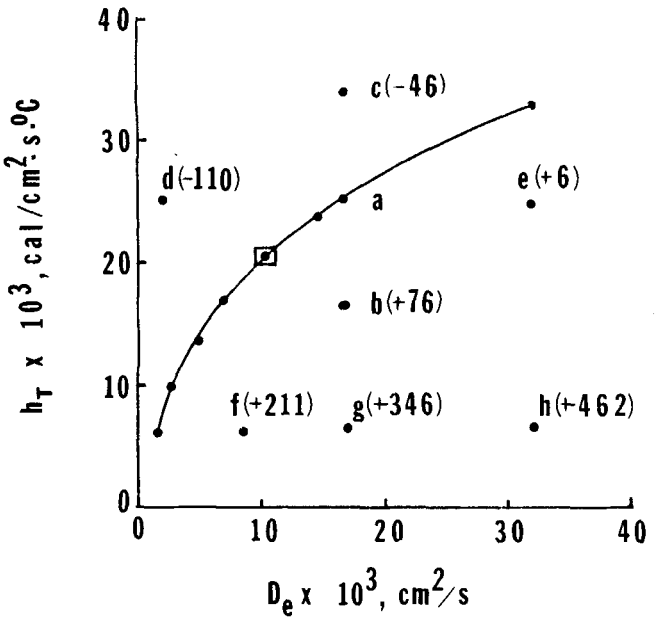

Fig. 9. Steady state parameter analysis for D_e and h_T, run 6U1.

pellet on introduction of uncontaminated feed in light of the information from 1 and 2.

Our discussion here will be centered primarily on points 1 and 3. The general approach has been to attempt a priori simulation, starting with a parameter set determined from off line experiments and steady state data, to use steady state analysis of the fresh particle behavior to determine whether or not the set is satisfactory for simulation, and finally to simulate the transient cases.

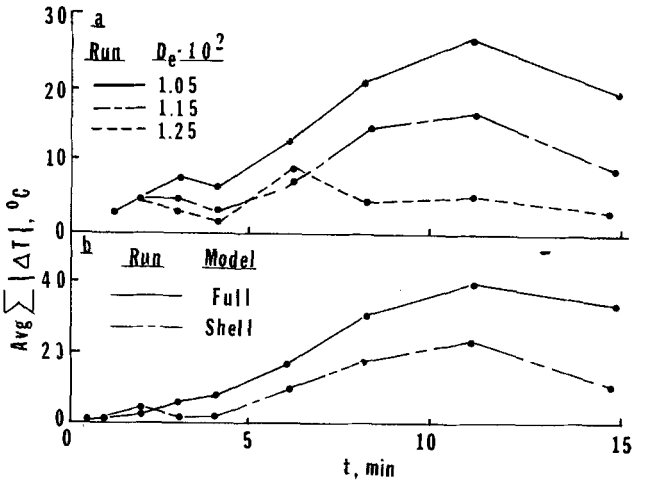

Fig. 10. *a.* Optimization of steady state parameter set on transient data, run 6U1. *b.* Comparison of full and shell models for 6U1.

Fresh, Undiluted Pellet

Run 6U1, Table 4, is representative of the behavior of the fresh, undiluted pellet. Steady state conditions for this run were an intraparticle temperature of 189°C, benzene conversion of 7%, and response time on start-up to steady state of approximately 20 min. Start-up data for this experiment are shown in Figure 8. A parameter set (D_e = 1.72 × 10^{-2} cm^2/s, λ_e = 17.6 × 10^{-4} J/cm-s-°C, h_T = 28.5 × 10^{-4} J/cm^2-s-°C, and k_g = 2.13 cm/s) was obtained from both separate experimentation and steady state data from the run. However, use of these values in the simulation resulted in a steady state intraparticle temperature 346°C greater than that measured experimentally.

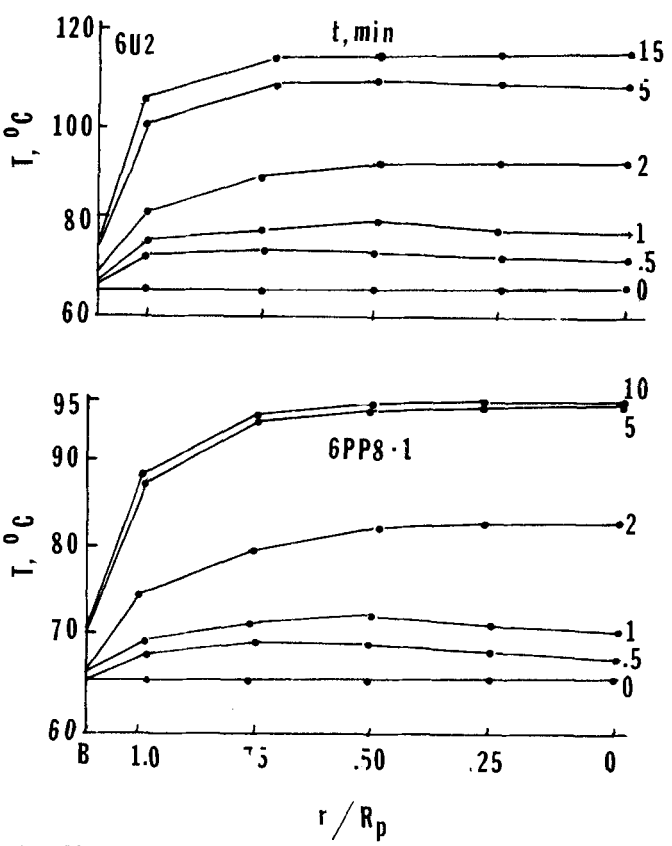

Fig. 11. Start-up response for the deactivated, undiluted pellet at two levels of global activity.

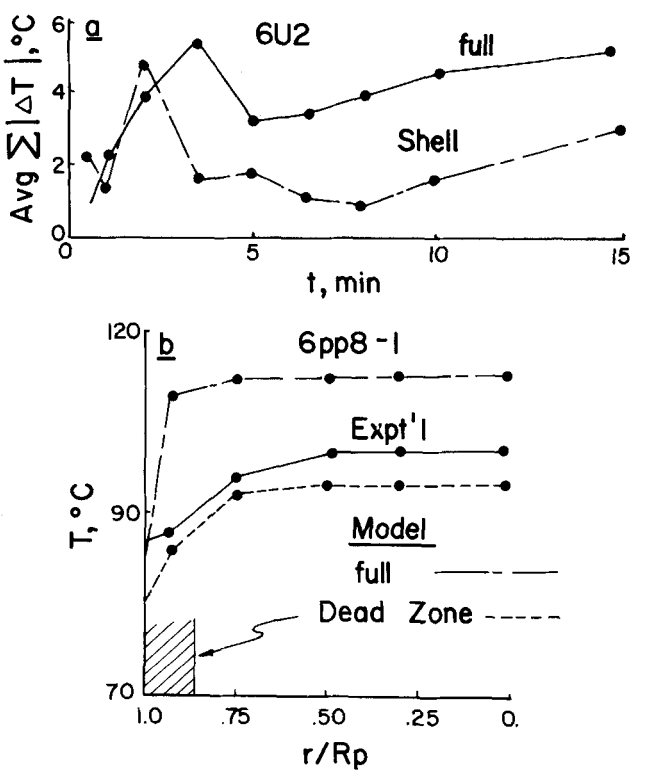

Fig. 12. *a.* Average temperature deviations for simulation of partially deactivated (S = 0.40) pellet. Parameters as for Figure 10. D_e = 1.05 × 10^{-2} cm^2/s. *b.* Comparison of temperature profiles computed via full and dead zone models for a severely deactivated (S = 0.16) pellet.

In view of this sensitivity, a one-parameter variation study was carried out to investigate the influence of each value individually. The parameters were identified in order of decreasing sensitivity as h_T, D_e, k_g, and λ_e. Subsequently, a two-parameter variational analysis was carried out by fixing the two parameters of lowest sensitivity at their original values and identifying ordered pairs of D_e and h_T which would result in a computed steady state temperature profile with a maximum $\pm 1°C$ deviation at any point from the experimental profile. The result of this exercise is given by the solid line in Figure 9, from which it is clear that there are many sets of parameters which will produce the given level of fit. The maximum deviation for some other D_e-h_T combinations is also shown in the figure, illustrating that such deviations are highly nonlinear functions of position in the D_e-h_T plane. The discouraging fact emerging from this study is that not only must some correct parameter set be identified, but the individual elements must also be determined very accurately. Is this possible? For example, the diffusivity values in Table 1 obtained from various sources such as the Prater relationship or counterdiffusion experiments agree to better than order of magnitude yet in the present instance yield values of h_T differing by approximately 30% (points b and c, Figure 9).

For transient simulation, the basis used for determination of a parameter set was the diffusivity from point *a*, determined from analysis of steady state data via the Prater relationship. The criterion for good fit employed here is the average of the absolute magnitude of the sum of deviations between measured and calculated temperature profiles at the points of measurement as a function of time. This form is limited in that it is not directly correlated with correspondence in the shapes of the profiles and does not indicate whether simulation lags or leads the experimental transients; nonetheless, it is sufficient for our present purposes.

Various pairs from Figure 9 were used in simulation of the transient results of run 6U1; all were found to give acceptable fits but with small variations among them. Since these are steady state values being used for transient simulation, further improvement might be obtained by variations on the steady state set. This is indeed so, as shown in Figure 10*a* for relatively small variations in the base diffusivity of 1.05×10^{-2} cm²/s from Figure 9 (enclosed point); however, the improvements are relatively modest (at least in comparison to the original discrepancy of 346°C), so in subsequent comparisons here we retain the steady state parameter set.

A final comparison for the undeactivated, undiluted case was the evaluation of a shell reaction zone model. The computed concentration profile vs. time for this run indicated only shallow penetration of benzene within the particle, about 0.1 cm maximum from the surface. Figure 10*b* gives a comparison for the full model ($s = 1.0$ for all r) and the shell model $s = 1.0$ for r within 0.1 cm of R_p, $s = 0$ for smaller r). The shell model is the equal, even superior in this case, of the full model and of course requires far less computer time.

Deactivated, Undiluted Pellet

Runs 6U2 and 6PP8-1 of Table 4 are start-up experiments on the undiluted pellet at two levels of activity, 0.40 and 0.16. Experimental data are shown in Figure 11. The parameter set obtained for the undeactivated catalyst (Figure 10) was used for simulation of these two deactivated pellets. Transient response results are illustrated for 6U2 in Figure 12*a* and steady state profiles for 6PP8-1 in Figure 12*b*. As indicated in the figure, either the full model, using the activity profile resulting from simulation of on stream poisoning, or a dead zone model was satisfactory. In the latter case, a dead zone ($s = 0$) of thickness 0.10 cm next to the external surface was incorporated into the full model, with $s = 1.0$ throughout the rest of the pellet. The dimension of this dead zone are in approximate agreement with results obtained via scanning electron microscopy for these pellets (Lee et al., 1978).

A word of caution is appropriate at this point concerning the interpretation of the global activity variable S. Recall that this is defined simply as the ratio of the overall rate of reaction of the deactivated pellet to that for the fresh pellet. Hence, the value of S reflects not only the loss of intrinsic activity of the pellet but also the concomitant reduction in the magnitude of the intraparticle temperature and thus the rate of reaction. The activity variable s appearing in the simulation model may indeed be a quantity much closer to unity than one might infer from the measured global activity; it is for this reason that the severely deactivated pellet of 6PP8-1 can be simulated adequately with a relatively small dead zone near the surface and unit intrinsic activity elsewhere.

Diluted Pellets

The same methodology in simulation was employed for the diluted pellets. For the graphite diluted catalyst, runs NKG-F65, NKG-P65, and NKG-D65, the parameter set $D_e = 2.9 \times 10^{-2}$ cm²/s, $h_T = 4.69 \times 10^{-3}$ J/cm²-s-°C, $\lambda_e = 7.03 \times 10^{-3}$ J/cm-s-°C, and $k_g = 3.83$ cm/s was determined from steady state experimental data and separate experiment. As in the case of the undiluted pellet, this set was found to be unsuitable for simulation, so the heat transfer coefficient was again determined from the model on the basis of acceptable fit. The average temperature deviations for typical simulations are given in Figure 13; parametric values employed are as above with the exception of h_T, which, at 1.67×10^{-2} J/cm²-s-°C, is about four times greater in absolute value.

For simulation of NKS-F65, NKS-P65, and NKS-D65, the initial parameter set was $D_e = 4.7 \times 10^{-2}$ cm²/s, $\lambda_e = 18.0 \times 10^{-3}$ J/cm-s-°C, $h_T = 38.5 \times 10^{-4}$ J/cm²-s-°C, and $k_g = 3.06$ cm/s; once again, this was found inadequate for simulation. A best fit result for NKS-F65 with D_e and λ_e unchanged and the heat transfer coefficient as an adjustable parameter is shown in Figure 14*a*, where $h_T = 24.7 \times 10^{-3}$ and $k_g = 19.4$. We note in this case that the major discrepancies in the fit occur during the initial portion of the transient; a series of separate simulation to explore this point revealed that variation in h_T had only a small influence on this initial region but substantially affected the fit at or near the final steady state. This, in turn, suggests that perhaps the effective diffusivity value is overestimated, since this would correspond to a deeper penetration of benzene into the pellet ultimately resulting in higher temperatures during the initial response. Accordingly, a lower limit on diffusivity was established from the Prater relationship using the thermal conductivity of the original parameter set and the steady state experimental profile; from this, $D_e = 1.7 \times 10^{-2}$ cm²/s. The resulting fit to the NKS series is shown in Figure 14*b*; parameters other than D_e are unchanged from Figure 14*a*.

Discussion

Clearly, the question which arises from these computational results is why the independently determined parameter values are apparently inadequate for the simulation. The particular sensitivity to variations in the heat transfer and diffusion coefficients is not surprising (although the magnitude is), since it has been suggested

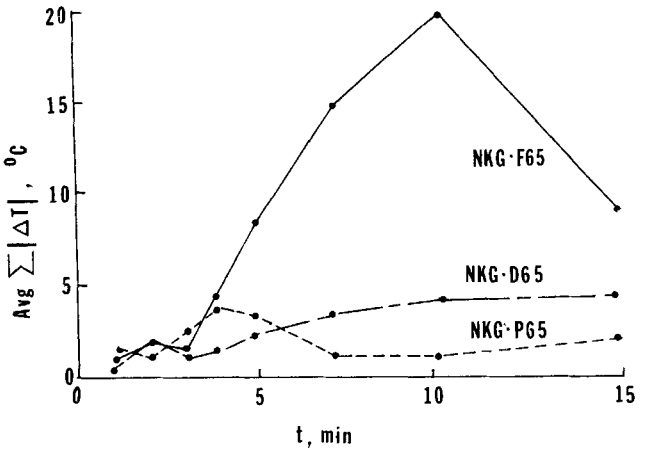

Fig. 13. Simulation results for low temperature runs, graphite diluted catalyst.

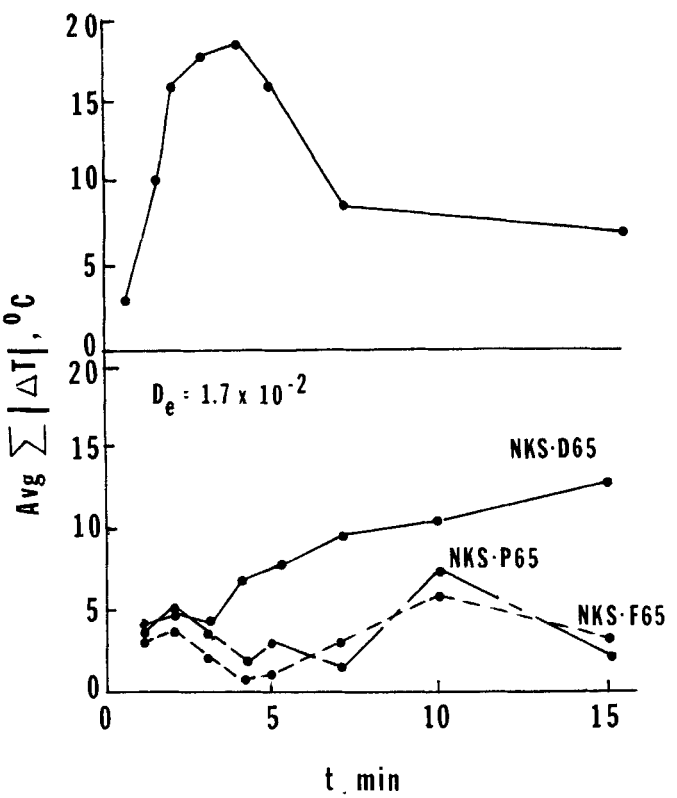

Fig. 14. *a.* Average temperature deviation, NKS-F65, initial simulation. *b.* Simulation results for low temperature runs, silica diluted catalyst.

many times that the major concentration resistance resides within the particle while the major thermal resistance is found in the external boundary layer. Although the external mass transfer coefficient varies in proportion to the heat transfer coefficient according to Equation (15), in no case investigated here was the external concentration gradient significant, and simulations are essentially independent of k_g values.

The discrepancies between the values of the parameters determined independently and those suggested by simulation can be at least partially explained on the basis of a combination of individual measurement errors and pronounced parametric sensitivity. Further is the complication that the base parameter set, derived from steady state information, is being employed for the simulation of the extreme case of transient response represented by the start-up experiment. Small variations in effective diffusivity have a profound influence on such transients, since the reaction and deactivation processes in these experiments are essentially confined to a relatively small external shell, the dimension of which is controlled by the depth of penetration of reactants and poison into the pellet. Yet there is considerable discrepancy in values of effective diffusivity obtained by various methods, as shown in Table 1, so there appears to be a basic conflict between the requirements of the simulation in terms of the accuracy of such parameters and our current ability to estimate them. A final complication is that the transport properties of the particle which are of importance in simulation are those pertaining to the zone of reaction, while the measured values of D_e and λ_e obtained from various sources are volume averaged quantities based upon the total pellet properties. Any localized inhomogeneity leading to corresponding localized variations in transport properties would be an important source of discrepancy between computation and experiment, given the parametric sensitivity of the simulation.

CONCLUSIONS

Comparison of the behavior of the diluted catalyst pellets with the undiluted pellet case indicates that alteration of the internal diffusional characteristics is the principal effect of dilution, while the modification of thermal conductivity and specific activity per unit volume is secondary. Both silica and graphite diluted materials exhibited qualitatively similar deactivation behavior, and the patterns of transient response were not qualitatively altered by deactivation. Two basic simulation models were employed for analysis of the experimental results: a full model as detailed by Equations (11) to (13) and a simplified version employing a finite annular active zone at the surface of the pellet with an inert center core. Both are adequate for simulation of all cases investigated (fresh and deactivated, undiluted, and diluted) but only in the sense of parameter fit models.

The failure of a priori simulation in representing the experimental results here provides some rather stern lessons concerning the level of detail feasible in such modeling. The system is complex, involving the interactions of rates of reaction, transport and deactivation under unsteady state conditions, and parametrically sensitive. It would appear that global, averaged quantities such as steady state activity and overall rates of deactivation can be determined approximately using independently determined parameter sets; however, detailed simulation of transients as carried out here requires parameters to be known to a degree of accuracy beyond our current capabilities in measurement or estimation.

ACKNOWLEDGMENT

This work was supported by the National Science Foundation under GK-17200. Dennis M. Downing was the recipient of an Energy Traineeship for 1975-1977.

NOTATION

a = kinetic constant, s^{-1}
a' = surface to volume ratio for the pellet, cm^{-1}
b = kinetic constant, cm^3/mole
C_i = concentration ($i = B, C, T$), mole/cm^3
C_p = heat capacity of pellet, J/g-°C
D_e = effective diffusivity, cm^2/s
E = activation energy for hydrogenation kinetics, J/mole
E_D = activation energy for poisoning kinetics, J/mole
F = modified activation energy, $E - H$, J/mole
H = temperature dependence of benzene adsorption

constant, J/mole
$(-\Delta H)$ = heat of reaction, J/mole
h_T = heat transfer coefficient, J/cm^2-s-°C
j_D = j factor for mass transfer
j_H = j factor for heat transfer
k_d^0 = preexponential factor for deactivation, s^{-1}
k_g = mass transfer coefficient, cm/s
M_T = thiophene capacity term, mole/cm^3-cat
N_{Bi_h} = heat Biot number
N_{Bi_m} = mass Biot number
N_{Pr} = Prandtl number
N_{Sc} = Schmidt number
r = radial variable, cm
R_p = particle radius, cm
r_B = rate of reaction of benzene, mole/s-g
r_D, r_T = rate of deactivation or adsorption of thiophene, mole/s-g
s = activity variable in model
S = global activity
t = time, min
T = temperature, °C
ΔT_x = $T_s - T_0$, interphase temperature difference, °C
$(\Sigma|\Delta T|)$ = average temperature deviation function
λ_e = effective thermal conductivity, J/cm-s-°C
ρ = density, g/cm^3
Ω = observed overall rate of reaction, mole/s-g

LITERATURE CITED

Benham, C. B., and V. E. Denny, "Transient Diffusion of Heat, Mass Species, and Momentum in Cylindrical Pellets during Catalytic Oxidation of CO," *Chem. Eng. Sci.*, **27**, 2163 (1972).

Butt, J. B., D. M. Downing, and J. W. Lee, "Inter-Intraphase Temperature Gradients in Fresh and Deactivated Catalyst Particles," *Ind. Eng. Chem. Fundamentals*, **16**, 270 (1977).

Carberry, J. J., "Yield in Chemical Reactor Engineering," *Ind. Eng. Chem.*, **58**, 40 (1966).

———, "On the Relative Importance of External-Internal Temperature Gradients in Heterogeneous Catalysis," *Ind. Eng. Chem. Fundamentals*, **14**, 129 (1975).

Downing, D. M., "Experimental and Modeling Study of the Influence of Deactivation and Catalyst Dilution on a Non-isothermal Catalytic Pellet," Ph.D. dissertation, Northwestern Univ., Evanston, Ill. (1977). Available from University Microfilms.

Kehoe, J. P. G., "The Thermal Response and Kinetic Behavior of a Catalyst Pellet under the Influence of Diffusion," Ph.D. dissertation, Yale Univ., New Haven, Conn. (1971).

———, and J. B. Butt, "Kinetics of Benzene Hydrogenation by Supported Nickel at Low Temperature," *J. Appl. Chem. Biotechnol.*, **22**, 23 (1972*a*).

———, "Interactions of Inter- and Intraphase Gradients in a Diffusion Limited Catalytic Reaction," *AIChE J.*, **18**, 347 (1972*b*).

Koh, H. P., and R. Hughes, "Catalyst Temperature Profiles under Poisoned Conditions," *ibid.*, **20**, 395 (1974).

Lee, J. W., "Effects of Intraparticle Deactivation on Catalyst Performance," Ph.D. dissertation, Northwestern Univ., Evanston, Ill. (1976). Available from University Microfilms.

———, J. B. Butt, and D. M. Downing, "Kinetic, Transport and Deactivation Rate Interactions on Steady State and Transient Responses in Heterogeneous Catalysis," *AIChE J.*, **24**, 212 (1978).

Lee, J. C. M., and D. Luss, "Maximum Temperature Rise Inside Catalytic Pellets," *Ind. Eng. Chem. Fundamentals*, **8**, 596 (1969).

———, "The Effect of Lewis Number on the Stability of a Catalytic Reaction," *AIChE J.*, **16**, 620 (1970).

Prater, C. D., "The Temperature Produced by Heat of Reaction in the Interior of Porous Particles," *Chem. Eng. Sci.*, **8**, 284 (1958).

Wakao, N., and J. M. Smith, "Diffusion in Catalyst Pellets," *ibid.*, **17**, 825 (1962).

Manuscript received June 2, 1978; revision received December 4, and accepted January 11, 1979.

Steady Nonionic Countergradient Transport Through Membranes by Coupled Diffusion

R. H. NOTTER
Y. M. TAM
and
S. MIN

Department of Chemical Engineering
The Pennsylvania State University
University Park, Pennsylvania 16802

Coupled diffusion generated countergradient transport through membranes is analyzed by experimental and theoretical means. Membrane wedge interferometer experiments on an ethanol-water-cellophane membrane system show that net countergradient mass transfer of the less permeable component ethanol may be generated over a wide concentration range. A theoretical analysis of an idealized membrane separating two binary bulk solutions is developed to display further the major features of diffusional coupling effects, and good agreement between observed and predicted countergradient transport characteristics is shown.

SCOPE

A new technique for the study of steady state one-dimensional membrane transport has recently been presented by Min et al. (1976). In their experiments on the transport of ethanol and water across a cellophane membrane, it was shown that under certain conditions it was possible to generate net mass transfer of ethanol against its concentration gradient. The membrane wedge interferometer experimental system used by Min et al. (1976) involved no temperature or hydrostatic pressure driven flows, and the countergradient transport results for ethanol were ascribed to diffusional coupling effects due to the greater transport of water through the cellophane membrane.

In the present paper we delineate further experimental studies of countergradient transport in the ethanol-water-

Correspondence concerning this paper should be addressed to R. H. Notter, Department of Radiation Biology and Biophysics, University of Rochester, School of Medicine and Dentistry, Rochester, New York 14642.